Available online at www.sciencedirect.com
ScienceDirect
Sedimentary Geology 199 (2007) 29–49
Sedimentary Geology
www.elsevier.com/locate/sedgeo

Very high energy sedimentation (supratidal hurricane deposits) and Mid-Holocene highstand on carbonate platforms, Andros, Bahamas: An alternative view

Françoise G. Bourrouilh-Le Jan *

Laboratoire CIBAMAR, CInématique de BAssins et MARges, Université Bordeaux 1, Avenue des Facultés, 33405 Talence Cedex, France

Abstract

Twenty-eight ^{14}C dates were obtained from 90 cores drilled through the tidal flats of western Andros Island, a large area ($2000\ km^2$), mostly covered by mangroves and stromatolitic deposits. These dates are correlated with location of the samples, sedimentological description, position of the samples at the time of deposition and their present-day sedimentological position. Measurements were made on bulk algal sediments and location of the relative paleo-sea-level is inferred from paleobathymetric reconstructions.

On the basis of ^{14}C dates, I conclude that the whole area was flooded about 5000 years BP and then was covered by the subtidal greyish mud facies, rich in Peneroplids, in the area of Deep Creek (north of the study area), Pelican Creek and Wide Opening (southeast of the study area). The level of this paleo-Great Bahama Bank Sea continued to rise until 3500 years BP and then slowly fell asymptotically toward the present-day level.

Thick hurricane marks (aragonitic lime mud with Didemnids spicules, several cm thick), previously defined as hurricane trails, can be observed throughout the cores, from 2000 years BP onwards. From 2000 years BP onwards it seems that the modern physiography was already established, including tidal estuaries, channels and stromatolite-bearing swamps.

Paleogeographic maps and sections have been drawn, and accumulation rates calculated in the various sedimentological zones of the tidal flats of western Andros. These vary between 0.5 to 0.04 mm/yr.

The modern topography of the tidal flats was established by 2000 years BP; similarly, the modern geological features, controlled by a tropical climate strictly dependent on hurricanes, were already established by 2000 years BP and seem to have been initiated between 2500 and 2000 years BP.

Keywords: Hurricanes; Holocene; Sea-level highstand; Bahamas

1. Introduction

1.1. Objectives

In this paper I will describe additional features of the Bahama Bank area that can be attributed to the influence of tropical cyclones and hurricanes (Bourrouilh-Le Jan, 1998). This influence has been most intense during the last 2000 years. Building on that, I will also present a model for the middle to late Holocene (ca. 5000 years) sedimentary deposition on western Andros Island of the Great Bahama Bank. This envisions a higher stand of sea-level at about 3000 years BP followed by a slow fall to present sea-level. This higher sea-level has been documented in other parts of the world (Flood and

* Tel.: +33 5 40 00 88 23; fax: +33 5 40 00 88 77.
E-mail address: f.bourrouilh-lejan@cibamar.u-bordeaux1.fr.

doi:10.1016/j.sedgeo.2005.12.032

Frankel, 1989;Beaman et al., 1994; Baker and Haworth, 1997, in Australia, Fletcher and Jones, 1996; Grossman and Fletsher, 1998, on Hawaiian Islands, Jedoui et al., 1998 in Tunisia, Blum et al., 2001 in Texas), despite the generally accepted curve for North American Atlantic coast and the Gulf of Mexico (Curray, 1960; Shepard, 1963; Scholl et al., 1969; Frazier, 1974; Belknap and Kraft, 1977; Parkinson, 1989; Thomas, 1990; Toscano and Lundberg, 1998; Rodriguez, 1999) and for Australia (Thom and Roy, 1983; Woodroffe et al., 1990).

The results of radiocarbon dating of a set of cores collected from carbonates deposited in the mangroves of western Andros Island adds to a series of studies carried out in the same region on sedimentology and diagenesis (dolomitization) of the mangroves, and, of the hydrology and diagenesis related to hurricanes (Bourrouilh-Le Jan, 1973, 1978, 1980, 1982, 1990, 1998).

The questions to be raised are the following: (1) has the dolomitized supratidal mud been deposited by slow Holocene sea-level rise, as Bahamian tidal flat histories are usually presented (Hardie, 1977), under the control of a sea-level that began lower than the present (Scholl et al., 1969; Pardi and Newmann, 1987; Gornitz and Seeber, 1990); or, (2) have they been deposited under the control of a sea-level higher than the present followed by a fall to present level and affected by stronger hydrodynamic agents as a result of intensification of hurricanes?

Another objective of my paper is to alert workers in the Bahamian area to the possibility of alternative scenarios for relative sea-level effects over the Late Holocene.

As shown by Blum et al. (2001), a Mid-Holocene highstand around many tropical, i. e. low latitude sites outside North America can have many causes: glacio- and hydro-isostatic crustal deformation (Clark et al., 1978; Clark and Ligle, 1979; Nakada and Lambeck, 1988; Tushingham and Peltier, 1991; Lambeck, 1993; Fleming et al., 1998; Peltier, 1998). In addition, changes of sea-level during Middle to late Holocene could also be related with paleoclimate changes during the same period between 5.7 to 3.2 ka (Denniston et al., 1999), or as recorded in ice core and other records (Dechamps et al., 1988; Stuiver et al., 1995; Bond et al., 1997; Zhang et al., 2000; Moustafa et al., 2000), specially changes in Antarctic ice volume (Sowers et al., 1993; Goodwin, 1998; Ingolfsson et al., 1998; Leuschner and Sirocko, 2000), with thermal expansion of the ocean waters as revealed by satellite altimetry (Chen et al., 1998; Minster et al., 1999; Cazenave, 1999). This higher stand of Mid-Holocene sea-level could explain peculiar sedimentological observation such as the disappearance of branching corals (*Acropora*) between 3030 and 3005 Cal BP in the Caribbean province) demonstrated by Hubbard et al. (2005) or the bank-top transition from non-skeletal- to skeletal-dominated deposition around 3.8 ka and a contemporaneous change in the abundance of transported allochems as observed by Dix and Kyser (2000). A middle Holocene relative sea-level highstand, estimated at 2 m above present mean sea-level, has been also pointed out in Mississippi Delta (Curray, 1961; Nelson and Bray, 1970; Penland et al., 1991; Törnqvist et al., 2004).

1.2. Previous work

Detailed sedimentological studies of the Andros Island area were carried out by Ginsburg and Hardie (1975), and then by Hardie (1977). Lowenstam and Epstein (1957), Neumann and Land (1975), Steinen et al. (1988), Macintyre and Reid (1992), Milliman et al. (1993), Friedman (1994), Milliman (1994), Robbins et al. (1997), concentrated their discussions on Bahamian aragonite mud origins. Gebelein and Hoffman (1973), and Gebelein (1974, 1975, 1977, 1978), Gebelein et al. (1980) and Rankey (2002) focused on the tidal flat of western Andros.

In other studies of the Bahamas, Newell and Rigby (1957), Newell et al. (1959), Cloud (1962), Shinn et al. (1965), Traverse and Ginsburg (1966) and Boardman et al. (1989) used bulk material for radiocarbon dating with success. Their work tabulated sedimentation rates on the Great Bahama Bank, and also recorded a number of ancient Holocene dates for the supratidal and intertidal sediments of the tidal flats.

The author has studied Bahamian carbonate environments and deposits for a number of years (Bourrouilh-Le Jan, 1974a,b, 1976, 1978, 1980, 1982, 1990, 1998), and that work forms part of the basis for the present paper. Some terms used below are detailed in her previous work as noted in the discussion.

1.3. Location, climate and environments discussed

Located between 24°20 N and 24°50 N, and 78° W and 78°30 W, the tidal flat covers an area of approximately 50 km × 40 km (Figs. 1, 2). Rainfall can exceed 50 mm per day during eight months of the year and up to 160 mm per day during four months. It causes important dilution in the surficial water bodies of the tidal flat (Bourrouilh-Le Jan, 1979, 1980, 1981).

Around Andros Island, several broad sedimentary zones have been recognized, and are described in Table 1 after Bourrouilh-Le Jan (1990). Six present-day sedimentary facies can be identified in the area. These

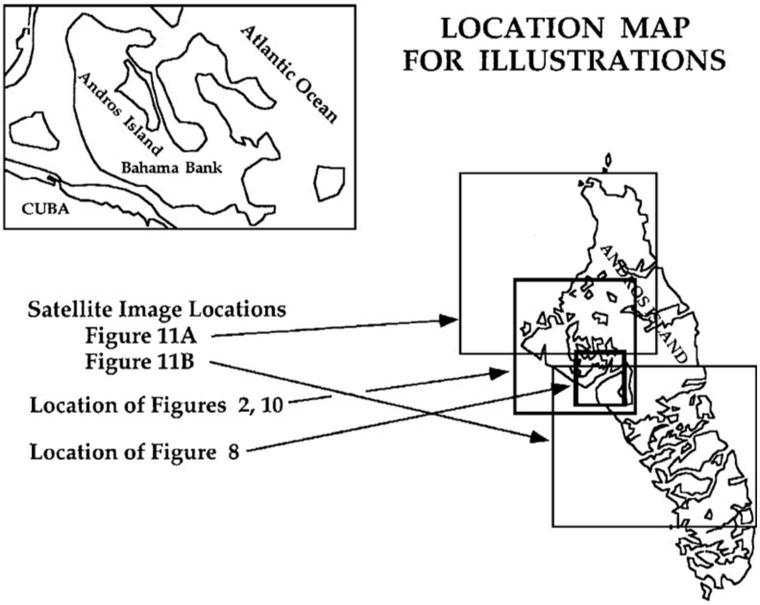

Fig. 1. Location of Andros Island on the Bahama Bank and areas illustrated in various figures in the text.

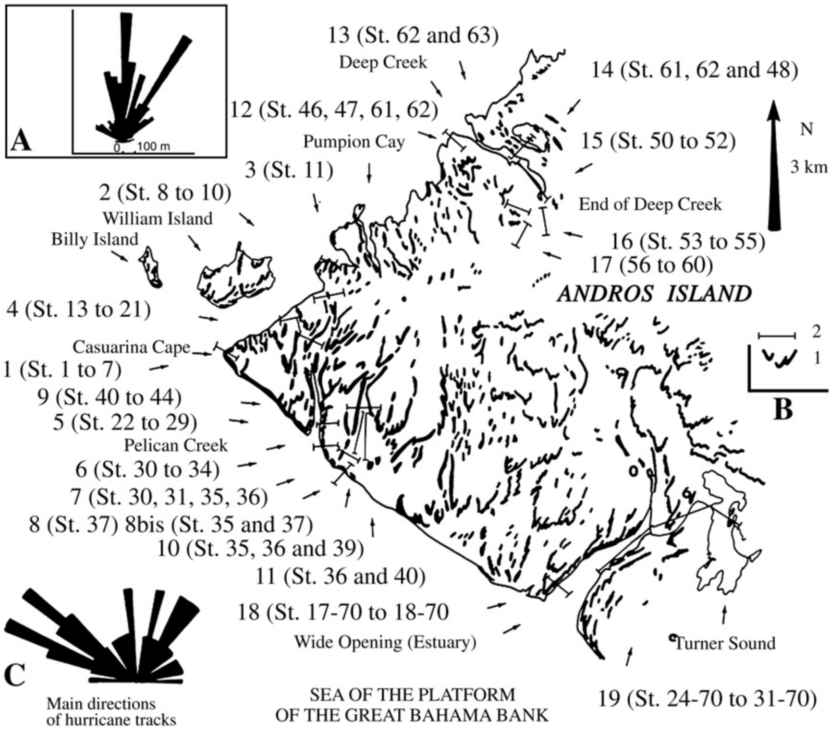

Fig. 2. Locations of stations, sections, and geographic localities in the northwestern portion of Andros Island. A: Main statistical trends and lengths of hurricane trails (hummocks), grouped at 5° intervals. B: Patterns of hurricane trails, drawn from vertical aerial photographs. C: Wind rose shows range of directions of hurricane tracks (from Cry, 1965) since 1873, centered on the western cape of Andros on a 100–200 km diameter area (Bourrouilh-Le Jan, 1998).

Table 1
Sedimentary zones of Andros Island (after Bourrouilh-Le Jan, 1978, 1990, 1998)

Zone	Description
Middle and southern zone, Great Bahama Bank	"Carbonate factory", mainly biological carbonate production (Lowenstam and Epstein, 1957, Purdy, 1963, etc., see text).
Southwest coastal subtidal talus zone	Lime mud, the zone of mud storage.
South-southwest coastal band	50 km wide, the zone of accumulation, numerous filled estuaries.
North-northwest coast	The zone of draining of cyclonic overflow, numerous channels and inlets (see Bourrouilh-Le Jan, 1998).

See also Figs. 2 and 3.

and their characteristics are tabulated in Table 2. Identification of these various zones and facies in sediment cores (Fig. 2) provides the data upon which this paper is based.

The deposits of the various zones are altered by the chemistry of the water saturating or adjacent to them. The character of these fluids can induce early dissolution of aragonite (Bourrouilh-Le Jan, 1980, 1998). The deposits are also altered by marine currents and cyclonic overflow that erodes earlier deposits of the north-northwest zone, which themselves are no longer built-up by hurricanes because of their position in the lee of the typical hurricane's path.

The tidal flat acts as a sediment filter during high-energy sedimentary events, such as hurricanes and tropical cyclones (Bourrouilh-Le Jan, 1978, 1998). These are common features of the Bahamian climatic regime.

1.4. Tropical cyclones and hurricanes

The Bahama archipelago is in the pathway of hurricanes and tropical cyclones of the North Atlantic. Hurricanes differ in scale from tropical cyclones and are defined as tropical depressions with winds higher than 118 km/h (74 mph) acting on a 1600 km diameter, and with heavy rainfall. Tropical cyclones and hurricanes are initiated in the equatorial zone, near the west coast of Africa (Cry, 1965; Neumann et al., 1978). Fig. 2 includes a wind rose for hurricane tracks which have been listed and drawn from the meteorological Bureau of Great Britain and the U. S. Weather Bureau, Washington D.C., in previous papers (Bourrouilh-Le Jan, 1978, 1980, 1982). In addition, this wind rose for hurricane tracks on the western part of Andros island explains the distribution of Pine pollens (Traverse and Ginsburg, 1966) and of whitings (Robbins et al., 1997) on the Great Bahama Bank, which are both localized north and northwest of Andros Island.

Detailed analysis of the western Andros Island tidal flats permitted identification of hummocks as hurricane-generated features, or "hurricane trails" (Bourrouilh-Le Jan, 1976, 1978, 1980, 1982, location of sections and samples in Fig. 2). The hurricane tracks wind rose (Fig. 2) coincides with statistical directions of morphologic axes of low hills colonized by Sabal palm trees (palm hummocks) of the tidal flats (Bourrouilh-Le Jan, 1978, 1982; Fig. 3), and covered by continental fauna and flora. Viewed from space, these weak topographic undulations appear as "V"-shaped sedimentary bodies, opening towards the northwest and northeast quadrant, and correspond statistically to hurricane paths that pass over Andros (see Fig. 11 later in text). Such features have been

Table 2
Present-day sedimentary facies which have been identified in the subject area

	Facies	Description
(1)	Subtidal estuarine facies	Grey or bluish muds (wackestone), numerous unlayered peneroplids (*Androsina lucasi*, Lévy, 1977), demonstrated to be subtidal on Andros Island and in Florida Bay (Lévy et al., 1988; Lévy, 1991). Never emerged because of their color, absence of dessication features, lack of diagenetic alteration (85% of aragonite, 15% of high Mg-calcite).
(2)	Intertidal estuary bank facies	Grey or bluish muds of estuarine facies, planar stromatolitic laminations, pellet layers or stromatolitic intraclasts.
(3)	Supratidal estuarine bank facies	Increase of planar stromatolitic laminations, first occurrence of very small cushion dome stromatolites, Mg-calcite lithoclasts.
(4)	Facies of cyclonic levees	Located several km from the Great Bahama Bank sea shore, surrounding fresh water ponds and the Sabal palm tree continental zone; thick lime mud beds (a few mm to many cm), 4% Ca-dolomite, dessication cracks, characterized by Didemnids spicules (Tunicates, Urocordea) from subtidal zone transported by hurricanes.
(5)	Bank facies of hyperalkaline lakes	Stacked stromatolites, pelletal beds with numerous mangrove leaves, interrupted by thick lime mud layers (5 to 8 cm) with Didemnids spicules, dessication cracks (hurricane marks).
(6)	Dry supratidal zone facies	Situated at great distances from the water line, stromatolitic laminations, intraclasts, bioturbation, pisoliths.

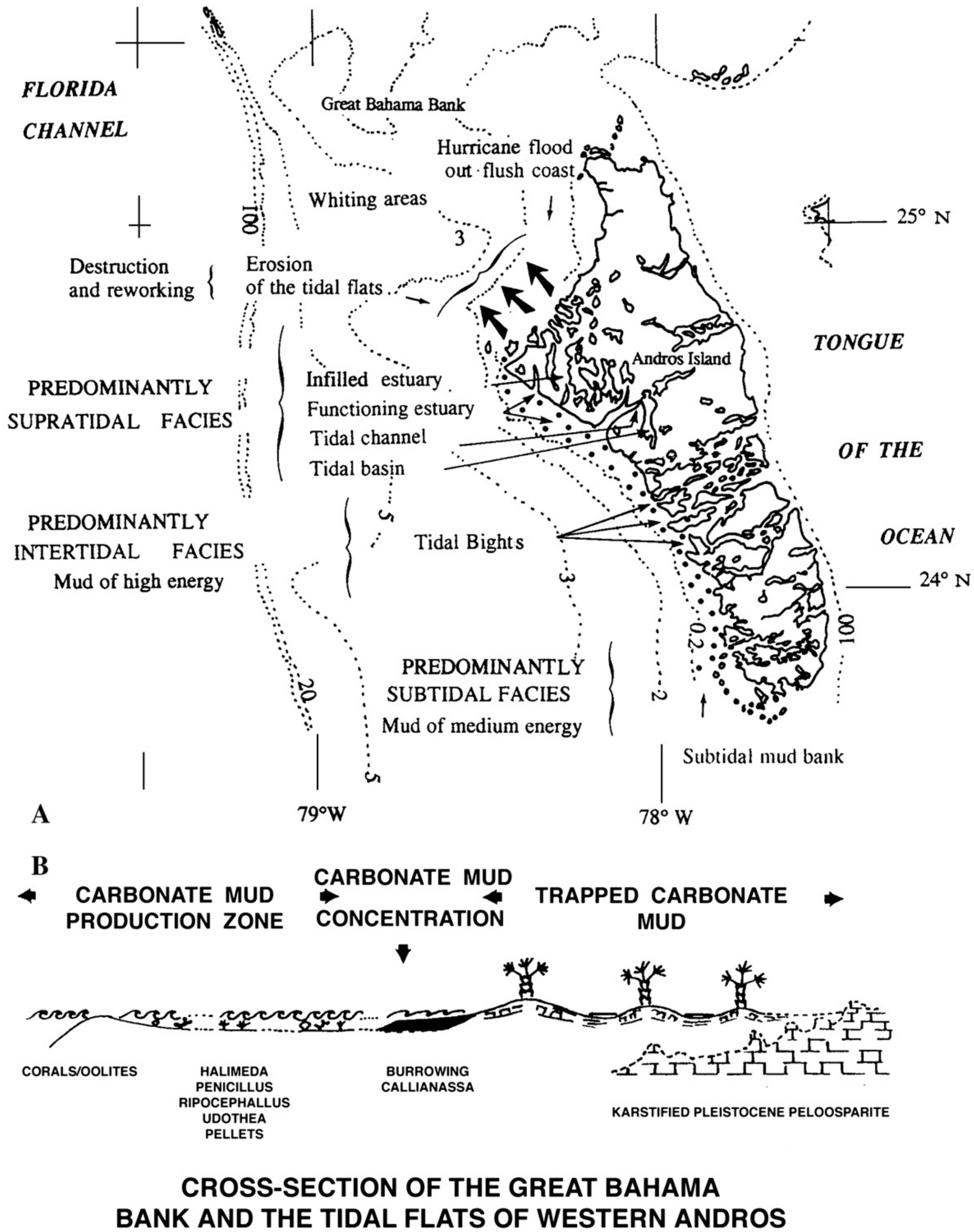

Fig. 3. A — Geometry of the sedimentary system of the western Andros tidal flats: a sub- to supratidal carbonate mud environment controlled by hurricanes. Bathymetry from hydrographic maps and satellite imagery. Dotted zone inside 0.2 m contour indicates zone of inter-hurricane stages with formation of subtidal mud banks. B — Schematic cross section of the Great Bahama Bank and the tidal flats of western Andros Island.

recently observed in the Pleistocene Bahamian interglacial substage 5e in different locations of the banks or in Bermuda (Hearty et al., 1998; Kindler and Strasser, 2000). These V-shaped sedimentary bodies are made by the pile-up of centimetric layers of cryptocrystalline aragonitic mud which become dolomitized with time (Fig. 4). So, the hurricane sedimentary action is scattered, scarce, discontinuous, with patches of few centimetric white mud layer on few square meters across the tidal flats and in relation with reworking of scattered ponds and tidal basins where cyanobacterial mats cannot develop and protect the mud from a hurricane disturbance. These supratidal muddy patches are visible in field (Bourrouilh-Le Jan, 1982, Figs. 3 and 4, and 1990) but cannot be seen through remote-sensing data (Rankey et al., 2004).

2. Control and accretion of supratidal sedimentary bodies in a carbonate environment by hurricanes

2.1. General statement

Geomorphic features of the Andros Island tidal flat which are controlled by high-energy climatic events, include "tidal estuaries", according to local English vocabulary, (Wide Opening, Pelican Creek, Deep Creek, etc.), tidal channels and basins, beach levees, lakes and

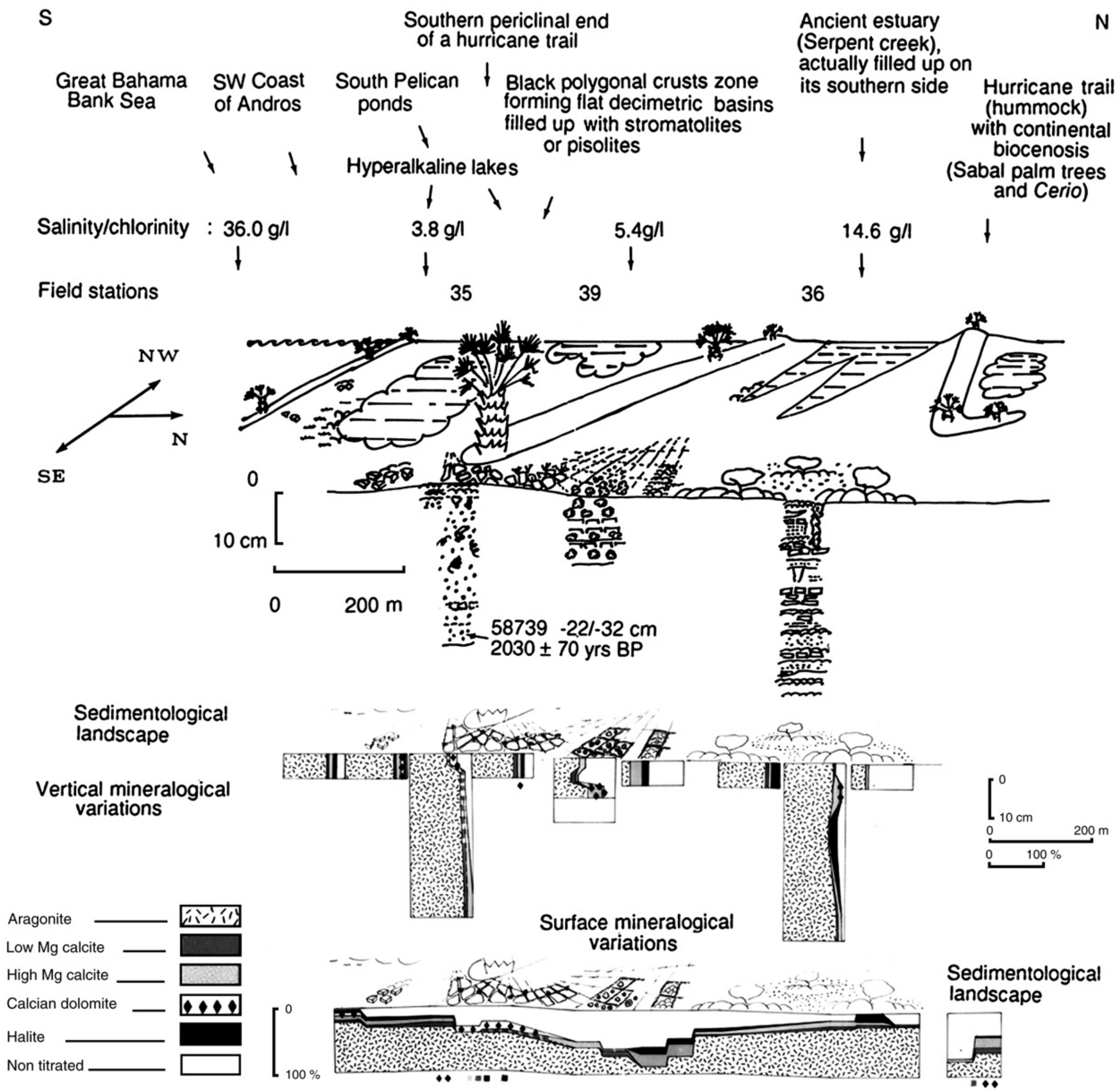

Fig. 4. Schematic cross section of hurricane trails, part of the predominant supratidal facies zone (example of cross sections 7, 8, 8 bis and 10 in Fig. 2; from Bourrouilh-Le Jan, 1990).

ponds, swamps and hurricane trails (Fig. 4). The tidal flat is covered by two main types of vegetation: continental Sabal palm forest and mangrove forests (*Rhizophora* and *Avicenia*) cover more than 80% of the tidal flat. The term "tidal basin" (Bourrouilh-Le Jan, 1978) refers to the vast mesohaline water tables of the tidal flat, linked to the sea by tidal channels of the Turner Sound type (Fig. 2). This term is synonymous with tidal lagoon used by Posamentier and Allen (1999).

Tropical hurricane marks, on Andros tidal flats, are made of several centimeters thick white aragonitic cryptocrystalline layers intercalated into stromatolite laminated sequences. Observed under polarized microscope and M.E.B, tiny calcitic spheroids can be recognized that have been identified as Didemnids spicules, belonging to the Urocordate or Tunicate phylum (Purdy, 1963). These spicules seem to have been interpreted in the literature, as calcitic precipitated crystals in the Bahamian whitings (Robbins and Blackwelder, 1992, D. Winston, personal communication 2005), or as spheroids produced by nannobacteria (Folk, personal communication, 1993, *in* Milliman, 1994).

Tropical hurricane marks are well developed on the stoss side of the hurricane paths (i.e., the southwest coast of Andros), and are altered by oligohaline and/or mesohaline waters in the northern area. Lines, tangentially traced from the points of the "V" shaped bodies formed by the cyclone tracks, correspond to morphologic lines inherited from Pleistocene sedimentary accretion, already observed on the east coast of Andros (Bourrouilh-Le Jan, 1974a,b). Therefore, the Pleistocene substratum has also influenced Holocene sedimentation during the initiation and the growth of hurricane marks.

On the stoss side of the hurricane paths, hurricane sedimentary trails are well-developed and preserved on the tidal flat, whereas, on the lee side of the hurricane paths, hurricane trails undergo erosion. Mechanical erosion occurs in the northwest direction due to the cyclonic outgoing surge, and chemical and biochemical erosion by dissolution takes place because of the mixing of fresh and salt waters on the tidal flat.

Lateral sedimentary cross sections (Fig. 4) have been compiled for several cores taken from several hurricane sedimentary trails (Bourrouilh-Le Jan, 1982, 1990). The cores characteristically show a subtidal facies at the base, followed by alternating lake and tidal basin deposits with thick laminations of hurricane and/or tropical cyclone origin whose diagenetic conditions vary from a humid (lacustrine or marine) to a dry environment (Table 2, Fig. 4). The surface and the internal structure of the "V" shaped sedimentary bodies are also characterized by various sedimentary features: teepees, stromatolites and pisoids. Paleosols are interbedded with the other facies.

The deposits of the mangrove environment may evolve as a result of either complete dessication (south-southwest coast, close to the source), or be eroded by dissolution or mechanically by hurricane flood retreat (north-northwest coast).

2.2. Tropical high-rainfall tidal flats and early diagenesis of dolomite

Two types of water exist which may, or may not, be linked to the Great Bahama Bank Sea: (1) a tidal basin water body, linked to the Bank by an estuary and a tidal channel, as in the Turner Sound type (Figs. 2 and 3) with a salinity typically of 10–15 g/l (mesohaline water tables), and (2) permanent lakes, due to the high rainfall and accumulation between the hummocks, with salinities between 0 and 6 g/l (oligohaline water tables; Fig. 4). Analysis showed that these waters are alkaline and hypersodic with concentrations of Na^+ and Ca^+ nine times higher than seawater diluted to the same salinity (Bourrouilh-Le Jan, 1980); Sr^+ content could not be analyzed because sample volume were insufficient; (Sr^+ content presents a high concentration in the Andros Island East coast ponds, coming from the dissolution of the Pleistocene outcrops, Bourrouilh-Le Jan, 1998).

Climatic and hydrologic conditions lead to solution of aragonite deposits. They also lead to the hyperalkalinity of closed water systems related to dolomitization that takes place at the surface of the tidal flats (Bourrouilh-Le Jan, 1990).

3. Methods

Sedimentological analyses include core x-radiographs, thin sections (cores were sectioned and resin-impregnated), mineralogy (XRD) and geochemistry (UV emission spectrography, for 23 elements). Twenty-eight ^{14}C dates (Table 3) were obtained on inter- to supratidal facies of the tidal flat of western Andros Island. In order to compare the results with those of a more unequivocal marine environment, a date was obtained from a core located in one of the large tidal straits (Middle Bight) that cuts the island in two parts, allowing flow between surface waters of the Great Bahama Bank and seawater from the Tongue of the Ocean.

In a previous version of this paper two points were the focus of reviewers' comments and should be addressed before presenting the discussion of this study.

Table 3
General results: ^{14}Carbon dates of the cored sediments in the mangrove swamps of the tidal flats of western Andros Island (for localization see Figs. 1 and 2) with the following information: core number, depth in cm in the core, station number, ^{14}Carbon age B.P., sedimentological description with the corresponding fossil sedimentological location and modern sedimentological position of the core

Core N°	Depth in core in cm	Station	^{14}C dates in years BP	Sedimentological description	^{14}C dates facies	Modern sedimentological location	Average value of sediment thickness in cm	Rate of sedimentation cm/10^3 yrs	Laboratory N°
58 186	−71/−78	25 (70)	5160 ± 140	Stomatolitic laminations with mangrove leaves	Intertidal mangrove marsh	In the tidal basin of the turner Sound, depth: −1.20 m	74	14.3	Ly-3104
58 183	−257/−263	18(70)	5050 ± 100	Mud with pellets, numerous gastropods and pelecypods	Estuarine subtidal	Wet mangrove marsh with black cyanobacterial mats. North Bank Wide Opening mouth	260	51.4	Ly-3102
58 190	−185/−190	30 (70)	5010 ± 120	Roots knotwork giving a peat (cf modern peat in East Andros coast ponds)	Brackish to lacustrine	Intertidal, south bank of Wide Opening, at the entrance of the tidal channel of the Turner Sound	187.5	37.4	Ly-3106
58 183	−150/−158	18 (70)	4080 ± 120	Pellets thin laminations	Intertidal estuarine bank	On the sandy levee on the N bank of the mouth of Wide Opening	154	37.7	Ly-3101
58 826	−67/−75	2bis	3000 ± 110	Gastropods mud	Subtidal Paleo-great Bahama Bank Sea?	In the wet mangrove marsh of Casuarina Cape (WNW cape)	70	23.3	MC-2584
58 186	−9/−19	25 (70)	2450 ± 110	Mud with pellets and Peneroplids	Modern sediments of the tidal basin of the Turner Sound	In the Turner Sound, water depth: −1.20 m	14	5.7	Ly-3103
58 372	−120/−123	32 (70)	2300 ± 120	Mud with fine marine bioclasts (spicules and small Foraminifera)	Same as now: “Tidal bight” of Middle Bight	Subtidal in a shallow tidal bight (Middle Bight)	122	53.0	Ly-3107
58 762	−28/−34	55	2180 ± 140	Grey mud	Estuarine subtidal	Estuarine intertidal bank (Deep Creek)	31	14.2	Ly-3113
58 726 b	−160/−185	22	2110 ± 60	Grey mud with Peneroplids	Estuarine subtidal	Estuarine intertidal bank (Pelican Creek)	170	80.5	MC-2586
58 732	−65/−75	28	2050 ± 60	Grey mud with Perieroplids	Estuarine subtidal	Mangrove marsh with fresh water hyperalkaline lakes (North Pelican ponds)	70	34.1	MC-2587

58 739	−22/−32	35	2030±70	White mud with Didemnids spicules	Hurricane mark	Dolomitization zone around hummocks	27	13.3	MC-2589
58 826	−1/−8	2bis	1810±70	Stromatolitic laminations with mangrove leaves	Mangrove marsh	Wet mangrove marsh with cyanobacterial mats	8	4.4	MC-2583
58 303	0	29 (70)	1700±90	White dolomitized dry polygons of mud	Supratidal: white mud with Didemnids spicules	Hurricane trail			GIF-3941
58 302	0	29 (70)	1630±100	White dolomitized dry polygons of mud	Supratidal: white mud with Didemnids spicules	Hurricane trail			GIF-2966
58 744 b	−44/−54	40	1575±60	Alternating mud with ostracods or gastropods	Estuarine subtidal	Intertidal: Remain of an estuary (Serpent Creek)	50	31.7	MC-2590
58 760	−20/−27	54	1460±110	Mud alternating with stromatolitic laminations	Estuarine intertidal	Supratidal (Deep Creek)	24	16.4	Ly-3111
58 747	−22/−26	43	1390±90	Supratidal, with dolomitic intraclasts	Supratidal	Supratidal (Serpent Creek)	24	17.2	Ly-3109
58 762	−2/−11	55	1310±110	Mud with Peneroplids and gastropods	Estuarine intertidal bank	Estuarine intertidal bank	7	5.3	Ly-3112
58 723 b	−65	19	1210±60	Grey mud with Peneroplids	Estuarine subtidal	Infilled estuarine bank	65	54.1	MC-2585
58 323	0	54	1090±90	White dolomitized polygons mud with Didemnids spicules	Supratidal	Supratidal in karstic small depression. East coast			GIF-3082
58 760	−2/−10	54	820±160	Stromatolitic laminations	Supratidal	Supratidal (Deep Creek)	6	7.3	Ly-3110
58 190	−1/−5	30 (70)	760±130	Mud with pelecypods and Peneroplids	Estuarine intertidal	Intertidal, Wide Opening, South bank at the beginning of the tidal channel to the Turner sound	3	3.9	Ly-3105
58 747	−2/−5	43	650±130	Stromatolitic laminations with dolomitized intraclasts	Supratidal	Supratidal (Serpent Creek)	3.5	5.3	Ly-3108
58 735 b	−40/−50	30	600±60	Grey mud with Perieroplids	Estuarine subtidal	Estuarine intertidal bank (Pelican Creek)	45	75	MC-2588
58 744 s	−6/−15	40	Modern (2,4% modern)	Mud with Peneroplids	Remains of estuary	Infilled estuary (Serpent Creek)	10		MC-2591

First, the validity of the dating which used bulk samples of aragonitic mud. In this study, the bulk samples were muds of a common algal or inorganically precipitated source and did not contain shell fragments, roots or other carbon sources. Therefore, the dates are based on essentially unit sources. These sampled materials are homogeneous and provide a common basis for dating and have previously been accepted for similar deposits (Macintyre et al., 1996). The pattern of the resulting dates also gave a coherent picture of age, depth and environment and did not produce scatter plots which would have been expected if significant mixtures of different source materials were present. Following Bard et al., 1998, a coincidence exists between calendar and noncalendar ages for the period 0 and 5000 years BP; in consequence the ages have been presented as non-calendar years, in years BP.

As noted earlier, additional radiometric dates were previously obtained in the same zone by Newell and Rigby (1957), Newell et al. (1959), Cloud (1962), Shinn et al. (1965), Traverse and Ginsburg (1966), and Boardman et al. (1989). These are examined together with my dates in the discussion.

Second, there were concerns that some of the materials in the carbonate muds, for example the Didemnid spicules (Tunicates) and Peneroplid tests (Foraminifera), live in a range of environments. This missed the point which is that the importance of these materials is in the fact that they were displaced and transported to higher levels. The author agrees that the importance of hurricane or tropical cyclone transport is primary and, in fact, is a key part of the paper. The question of the driving force that gave the effect of higher sea-level about 2000 years BP is an open one. It may have been an actual eustatic change, or the cumulative effect of a period of increased hurricane or tropical cyclone frequency, and perhaps intensity, that produced a stacking of hurricane tracks and the net movement of materials to physiographically higher positions.

4. Results

4.1. Mid-Holocene sea-level highstand

Radiocarbon-dated sediments (Table 3) from the tidal flat of western Andros Island were correlated with sample location, sedimentological description, position at the time of deposition and present-day sedimentologic position. The facies have changed little vertically and the dominant estuarine facies consists of grey mud with numerous subtidal Peneroplids (*Androsina lucasi,* Lévy, 1977), e.g. deposits in the estuaries of Deep Creek, Pelican Creek and Wide Opening. The physiography has changed greatly between 6000 years BP and 2000 years BP because of rapid relative sea-level rise, but shows little change from 2000 years BP onward.

The sample located 65–75 cm down-core (Fig. 4) taken from the fresh water ponds in the North Pelican ponds zone, yielded an age of 2050+/−60 years BP, whereas the top of the core (i.e. present topographic surface) is between 1 and 2 m in altitude. Therefore, if the 65–75 cm is subtracted from the present-day elevation, a value of +0.35 to +1.35 m above the

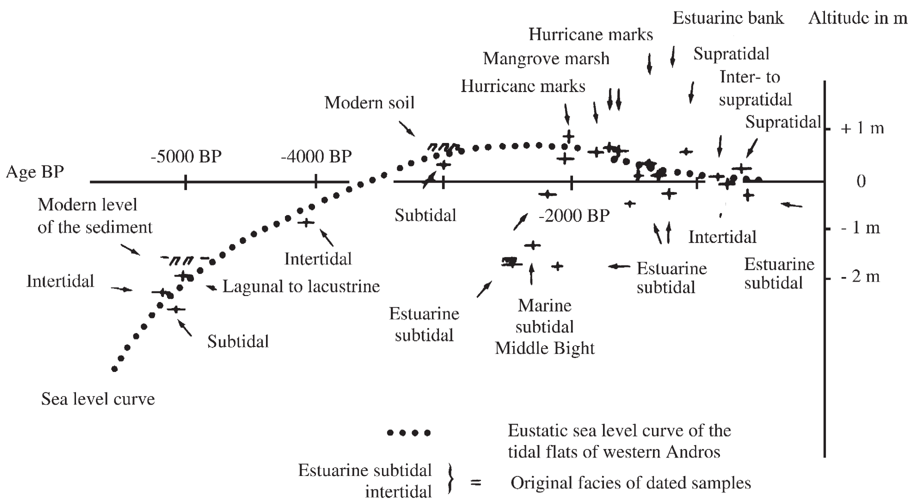

Fig. 5. Sea-level curve for the western Andros Island tidal flats. Original depositional facies are indicated and each sample is placed in time along the *x*-axis, and in space along the *y*-axis referenced to modern sea-level with error bar.

present-day level is obtained. The facies of this sample is a subtidal grey mud with *Androsina* (estuarine facies), which demonstrates that at the present-day location +0.35 to +1.35 m, there was in the past an estuary into which a subtidal facies was deposited about 2050 years BP, and which corresponds to a Mid-Holocene relative sea-level higher than at present. Quaternary workers have documented evidence for a higher Mid-Holocene stand in other areas (Beaman et al., 1994; Baker and Haworth, 1997, in Australia, Fletcher and Jones, 1996; Grossman and Fletcher, 1998, on Hawaiian Islands, Jedoui et al., 1998 in Tunisia, Blum et al., 2001 in Texas).

Similarly, a core sample (#58723b, Table 3) was dated at 1210 years BP for an estuary facies. This sample was taken 65 cm down-core, at which the present topographic surface is situated between 1 and 2 m, and this indicates the presence of a Mid-Holocene highstand sea-level situated from +1.35 to +0.35 m above present-day sea-level (Bourrouilh-Le Jan, 1993, 1996). These sedimentological observations allow the construction of the sea-level curve for western Andros tidal flats (Fig. 5), which points to a Mid-Holocene sea-level highstand around 3000 years BP.

4.2. Geomorphological stability, hurricanes and phreatic lens level

Fig. 5 shows that around 5000 years BP, sea-level was 2 m below the present-day sea-level. The geomorphologic features of the zone were already those of the present-day.

The oldest dates were obtained from areas of Wide Opening and Turner Sound and correspond to a typical marine facies. They indicate that near 5000 years BP Wide Opening already existed as an estuary, perhaps with a small displacement towards the south. Similar dates were obtained by Lidz et al. (1997) for the marine flood of the Floridan reef platform. Fauna included Foraminifera (Rotalids), Pelecypods and Gastropods without any evidence of inherited reworking, whereas the far end of Wide Opening was occupied by a peat lake, and Turner Sound was occupied by marine to brackish swamps with stromatolites.

In the middle of the tidal basin of the Turner Sound, the higher present-day upper surface of the sediment (−1.5 m) and the age of 5000 years BP for this facies at −0.71 to −0.78 m down-core, indicate that sea-level at that time was at approximately −2 m (Fig. 5).

The eustatic curve shows that around 5000 years BP, the hydrostatic level of the water table initiated the formation of the surficial peat, situated around −2 m to −2.5 m and that sea-level was probably close to that elevation.

Supratidal, dolomitized, thick polygons of lime mud with dessication cracks were dated at 1700 and 1630 years BP (Fig. 5). Their position on the curve confirms that these levels were in the intertidal zone or slightly supratidal during their genesis (they are in the upper level of the supratidal zone today).

This conclusion concerning date of formation and paleoenvironment of the dolomitic crusts is important in order to understand their diagenesis.

5. Consequences

5.1. Lateral variations in intertidal to supratidal facies

Shinn et al. (1965) dated nine samples: – a *Cerion*, gastropod shell, and – eight sediment samples (dolomite and a mixture of carbonates). But the date obtained on the gastropod shell (1690 years BP) that occurs below one of the sediment samples, was not taken into account by these authors. The following new interpretation (Fig. 6) is that: (a) there is a

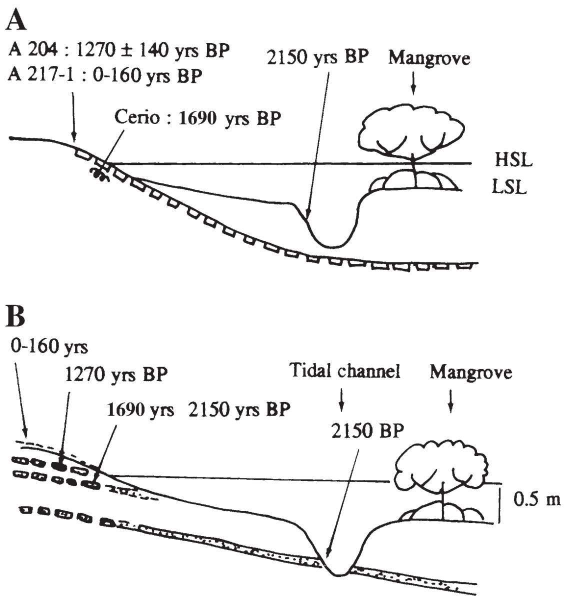

Fig. 6. Consequence of the Mid-Holocene highstand position: the position of the dolomitized zone: (A) interpretation and location of dolomitized zones according to Shinn et al. (1965). The dolomitic dry polygonal layer is continuous and overlain discontinuously by channel sediments. (B) New interpretation of this paper: the facies are continuous. The dolomitized polygon layer is the result of local supratidal diagenesis, located on the hummocks and their periphery, which are themselves controlled by high-energy sedimentation (hurricane trails, Bourrouilh-Le Jan, 1978). ^{14}Carbon dates as in (A).

continuity between the sediments and the dolomitic crust, and (b) — there are lateral variations of facies that are repeated vertically, the hummocks having always been in a high zone of the supratidal deposits (Fig. 6).

5.2. Rate of sedimentation: reduction of accommodation

According to Cloud (1962), the rate of sedimentation is 0.8 mm/yr for subaquatic muds of the Great Bahama Bank. The sedimentation rates in Fig. 7 appear as

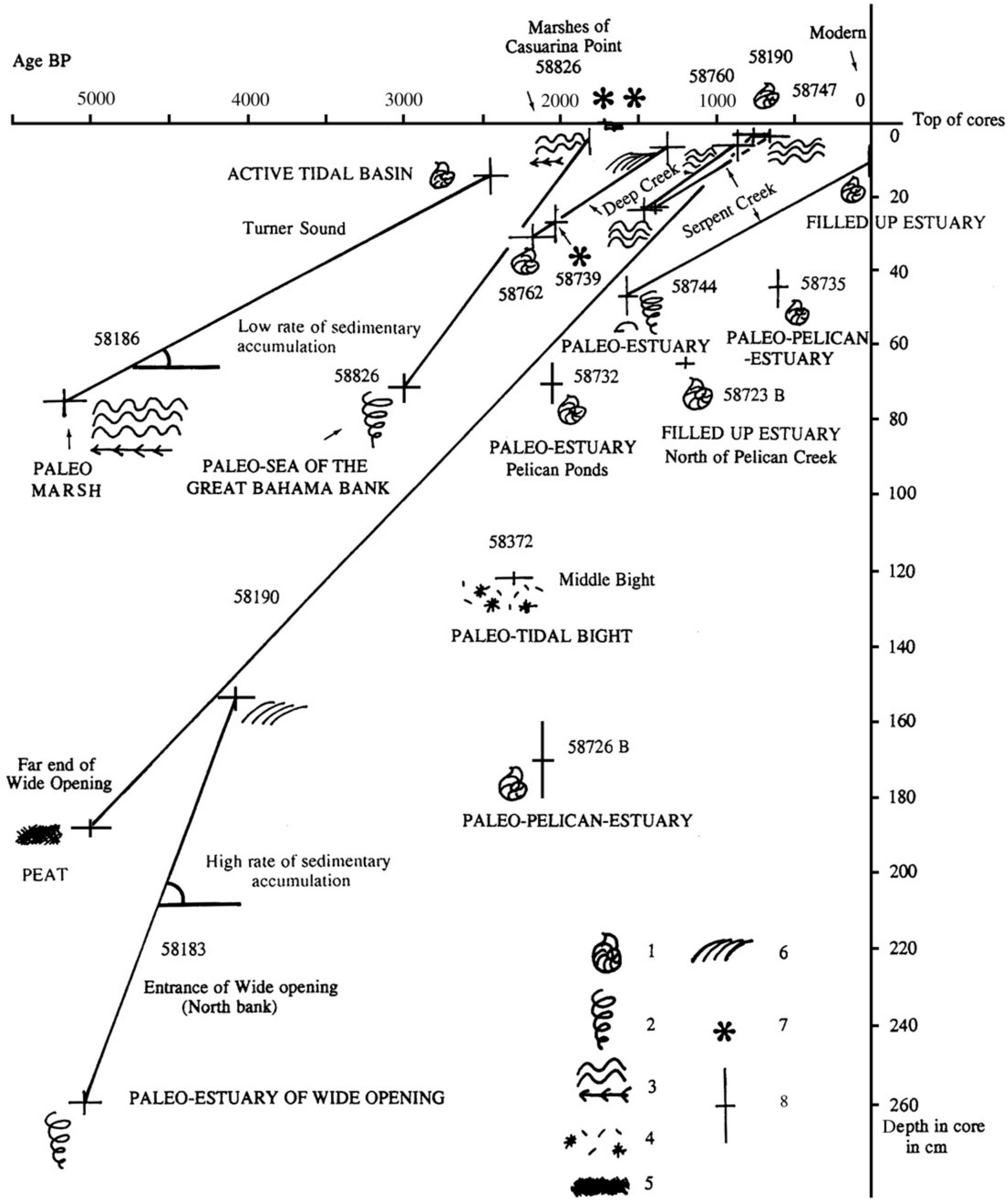

Fig. 7. Thickness of accumulated sediments versus ^{14}Carbon dates and paleofacies, considering cores one by one. Facies symbols are identified as: 1: Estuarine facies with Peneroplid *Androsina lucasi* (Lévy, 1977); 2: Paleo-sea deposits of the Bahama Bank: wackestone with marine gastropods; 3: Mangrove marshes facies: laminated stromatolites with mangrove leaves; 4: Mudstone with nannofossils (Didemnid spicules) from the high-energy mud accumulation from the Bights (Middle Bight); 5: Peat; 6: Tidal estuarine bank facies; 7: Supratidal facies: thick dolomitized mud with dessication cracks; 8: ^{14}Carbon dates with error bars.

straight segments because only two points are known for each curve of sedimentation rate according to each environment.

(1) All core data have the same general trend.
(2) The slope of each straight segment varies as a function of the position of the cores in the sedimentary system. In absolute values, the slope of the lines is steep, indicating a high sedimentation rate for core samples from estuarine deposits (e.g. Wide Opening, Deep Creek and from several remnants of estuaries). The cores from northern and southern Pelican ponds present the same types of rates and represent ancient estuary banks.
(3) The sedimentation rate decreases with time, for example in Section 1, dates were obtained on a core from mangrove swamps. The sedimentation rate for the period from 0–3000 years BP is 23 cm/1000 yr, and for the period from 0–1810 years BP, the sedimentation rate is 4 cm/1000 yr.

At the mouth of the Wide Opening tidal estuary on its north shore, the sedimentation rate is 51 cm/1000 yr at 5050 years BP and 38 cm/1000 yr at 4080 years BP. In the middle of Wide Opening, the rate is 37 cm/1000 yr at 5010 years BP and 4 cm/1000 yr at 760 years BP. Finally, in the middle of Turner Sound tidal basin, the rate of sedimentation is 14 cm/1000 yr at 5150 years BP and 6 cm/1000 yr at 2450 years BP.

Therefore, on the tidal flats of western Andros Island, there is a decrease in the rate of sedimentation through time that might be related with

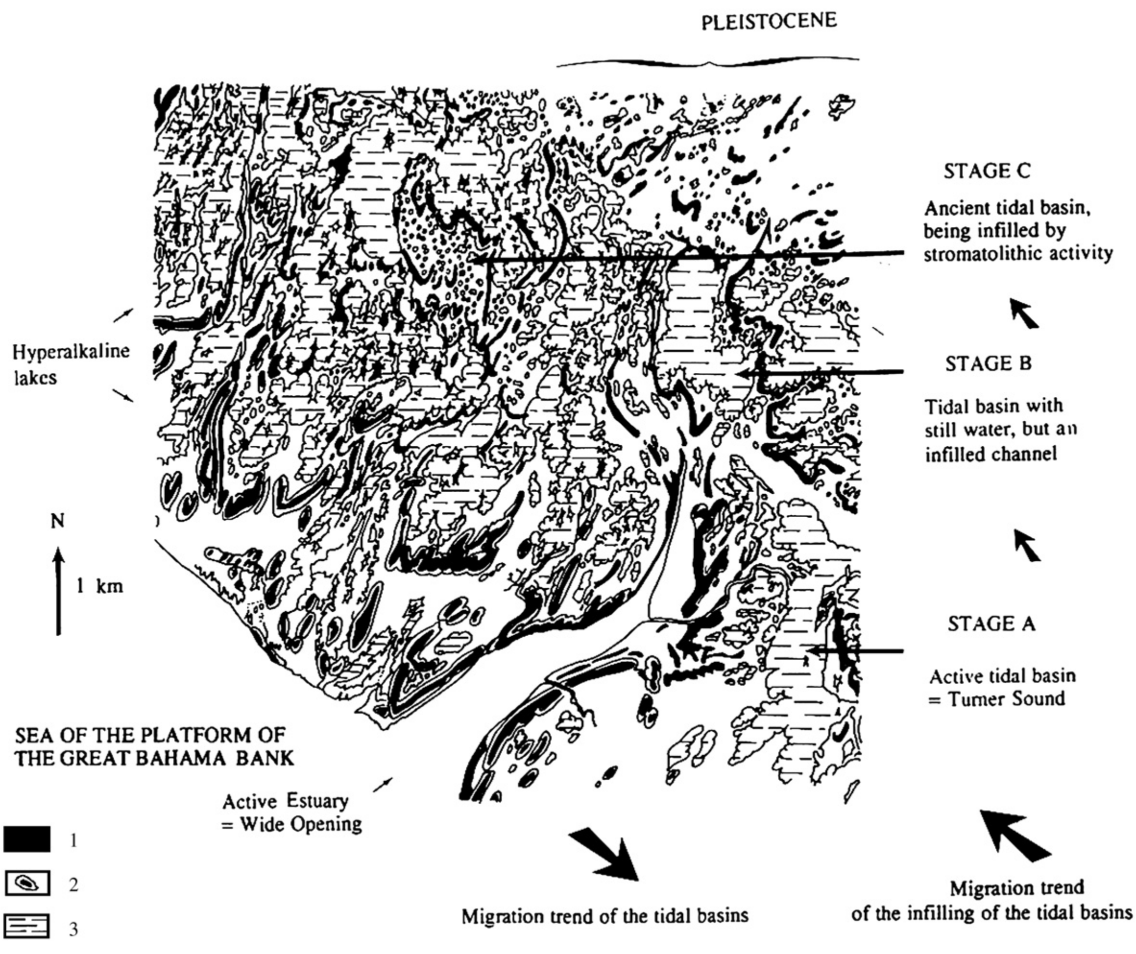

Fig. 8. Lateral evolution of the sedimentary system of the tidal flats of western Andros Island. This evolution is not only responsible for the building of the carbonate body, but also of its diagenesis. The evolution for the tidal basins is identical. Drawn from aerial photographs. Facies symbols: 1: Hurricane trails or hummocks, indicating continental and supratidal conditions. 2: Dolomitization zone. 3: Lakes, ponds and tidal basins.

the reduction of accommodation space due to a higher sea-level stand several hundred years before.
(4) For a given environment, this decrease is constant.
(5) The rate of sedimentation is much higher in estuaries and bights when the water level is linked to the sea (e.g. Pelican estuary and Middle Bight), confirming the major role of marine sources and not *in situ* precipitation of carbonates.

The main sedimentological observations are: (1) the sediments originate from the Great Bahama Bank, i.e. from the south and southwest; (2) the sediments are

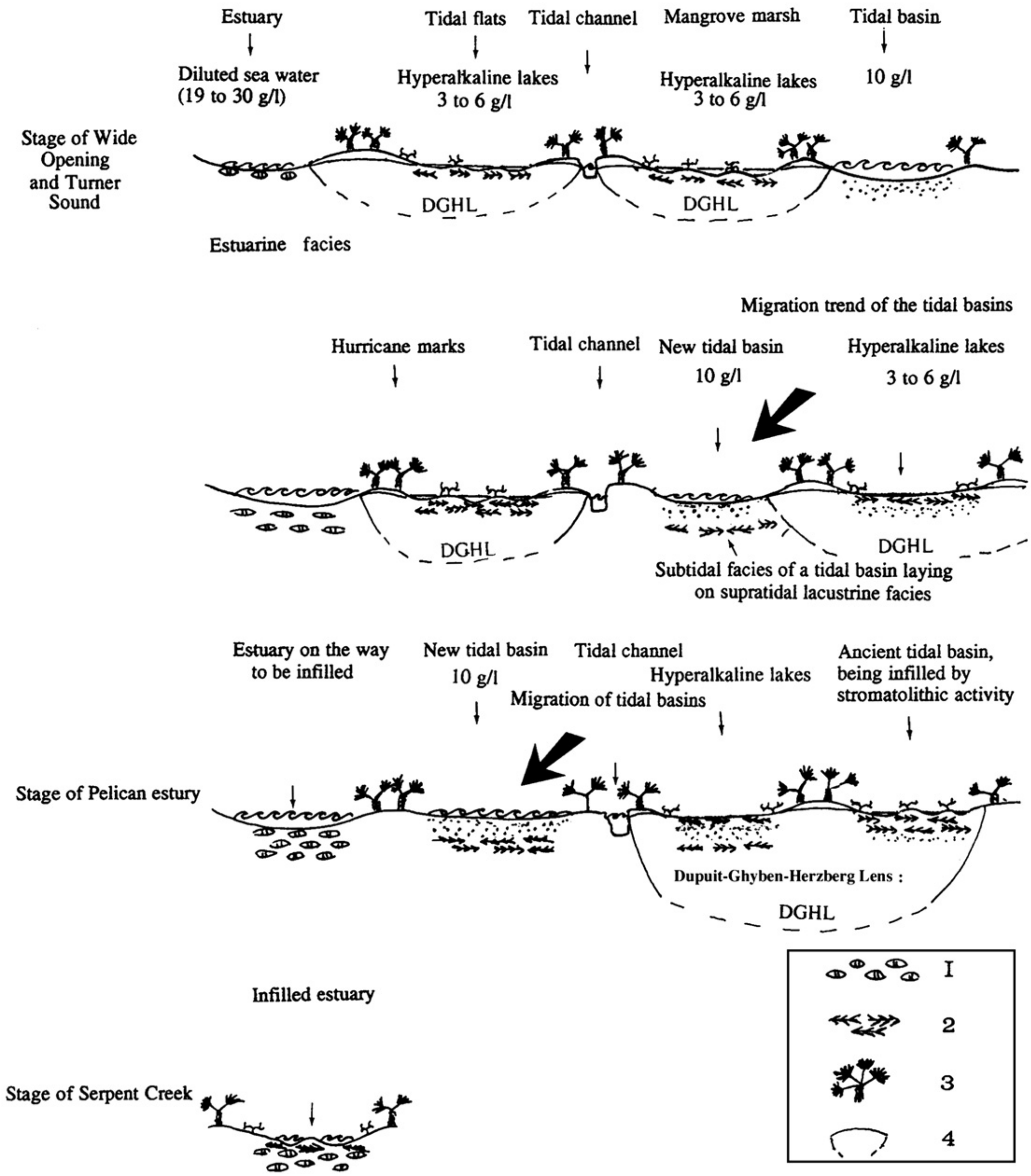

Fig. 9. Vertical evolution of the sedimentological system of the tidal flats of western Andros Island with lateral migration of the tidal basin, estuaries, channels and lakes, and the superposition of the corresponding facies. 1: Estuarine subtidal facies with Peneroplid foraminifera (*Androsina lucasi*, Lévy, 1977). 2: Dry and wet mangroves with hyperalkaline lakes and stromatolites. 3: Continental zone with hurricane sedimentary deposits. 4: Position of the fresh water phreatic lens (DGHL : Dupuit–Ghyben–Herzberg lens). The depth of the DGH lens is forty times the altitude of its upper level (Dupuit, 1848-1863; Ghyben, 1888–1889; Herzberg, 1901).

trapped along the coast of the tidal flat, just behind this coast, after being accumulated as a subtidal mud bank along this coast during inter-hurricane periods; (3) in consequence, there is only a small net quantity of aragonitic mud transported into Turner Sound tidal basin, despite the small marine deltas visible on aerial photographs.

5.3. Space and time evolution

5.3.1. Horizontal evolution of the tidal flat:

The sedimentological reconstruction from 18 horizontal cross sections throughout the tidal flats based on 90 cores shows that the general direction of evolution of the tidal flats is towards the south-southeast (Fig. 8). The sedimentological system of the tidal flats evolves through the following stages: first, they are functional and open (A); second, they become closed with waters of various salinities (B); and, finally, become totally filled (C). This evolution occurs for both estuary and tidal basin (Fig. 8). It can continue by returning to Stage A because of the influx of marine waters from the northwest. This result is new and disagrees with conclusions of previous authors. It confirms the general sedimentation map (Fig. 3). The general direction of sediment accretion is, therefore, south-southeast, whereas destruction and reworking take place to the north-northwest as indicated by relict zones or buttes such as Billy and William's Islands.

5.3.2. Vertical evolution (Fig. 9):

Facies location and evolution are also seen vertically: cores between hurricane trails present the following facies successions: estuarine facies (muds with Rotalids, aragonite and Mg-calcite), pond facies (stromatolitic laminations, pisoids, pellet beds, dissolution of aragonite), and supratidal facies (stromatolitic laminations with Mg-calcite). If the basin is flooded again, the influx of marine waters will logically lead to the reappearance of the estuarine facies (Fig. 9).

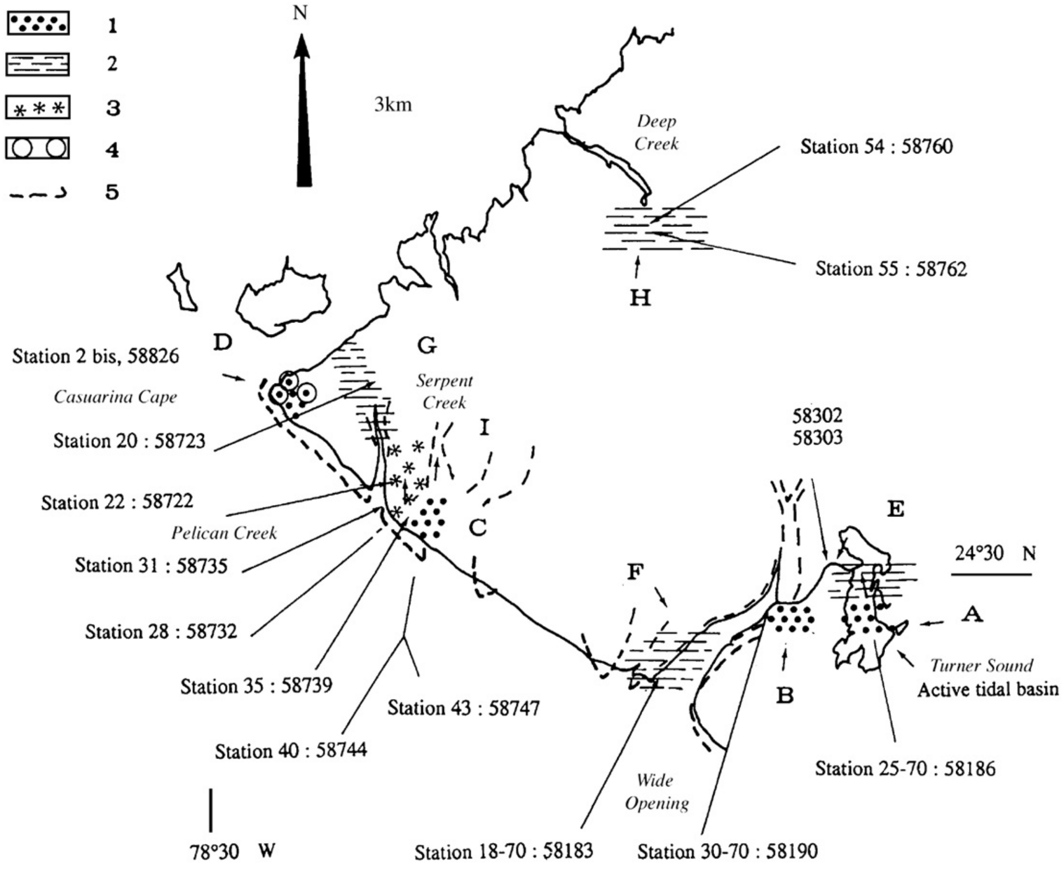

Fig. 10. Paleogeography and location of [14]Carbon dates of western Andros Island tidal flats based on the following main facies: (1) Marshy to lacustrine facies; (2) Subtidal estuarine facies; (3) Recent 1.8 m thick sediments, depositing as early as 2000 years BP, absence of dolomite; (4) Marine subtidal facies (Paleosea of the Bahama Bank); (5) Fossil coastline. Detailed explanations in text. Dates on Fig. 4 and Table 3.

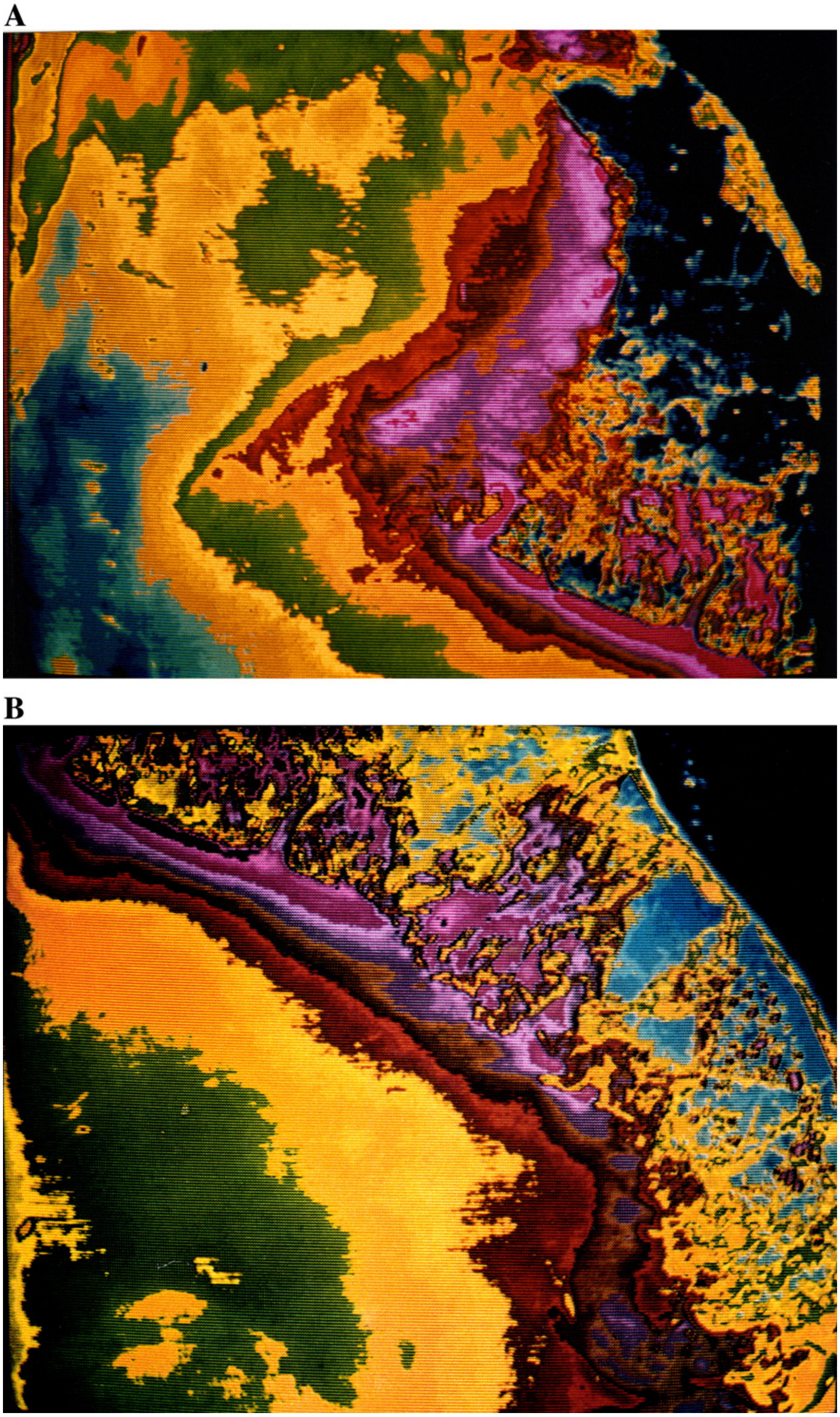

Fig. 11. Details of satellite imagery of Andros Island. False color images, channel IV, kindly contributed by TOTAL. (A) Northern part of the Bahama Bank and northwestern part of Andros Island: the carbonate mangrove exhibits an inter- to supratidal position. (B) Wide Opening area, the bights and the southern portion of Andros Island: modern carbonate mangrove zone with a sub- to intertidal position illustrating the geomorphology of the previous northwestern mangrove between 2000–3000 years BP. See Fig. 1 for area locations.

5.3.3. Mid-Holocene paleogeography of the tidal flats of Andros (Fig. 10):

The modern tidal basin of the Turner Sound area (Fig. 10, A) was marshy to lacustrine at 5160 years BP, while its channel mouth (B) was filled with brackish to lacustrine water at 5010 years BP. The northern bank of Wide Opening (F) shows subtidal estuarine facies at 5050 years BP and 4080 years BP. The Paleo-Sea of the Great Bahama Bank occupied the *Casuarina* Cape (west-northwest Andros Cape) with marine subtidal deposits at 3000 years BP (D in Fig. 10). In Turner Sound (E), the tidal basin regime (10 g/l) was formed with pellets and Rotalids, at 2450 years BP. *Casuarina* Cape area (D) became marshy to lacustrine at 1810 years BP. The far end of Deep Creek (H) was an active estuary at 1310 years BP, as was the northern area of Pelican Creek (G) at 1210 years BP. The area north and south of Pelican Creek pond zone (I) was filled with 1.8 m-thick sediments starting at 2000 years BP, and does not exhibit any dolomite. The modern sediment-filled and dry paleo-estuary of Serpent Creek (C) was marshy to lacustrine at 600 years BP.

Assuming a sea-level slightly higher than present-day, the tidal flat on western Andros Island 2000 years ago should have exhibited a paleogeography resembling the zone of present-day central Andros (aerial and satellite reconnaissance, Fig. 11A, B), i.e. the islands that form a “V” shaped body in a brackish environment where the estuarine facies are deposited.

Since 2000 years BP slow and progressive lowering of the sea-level, i. e. reducing accommodation space, has allowed the emersion of all the previously deposited facies while accumulation of a great quantity of mud was going on along the southwest coast of Andros. Very high energy events (hurricanes and tropical cyclones)

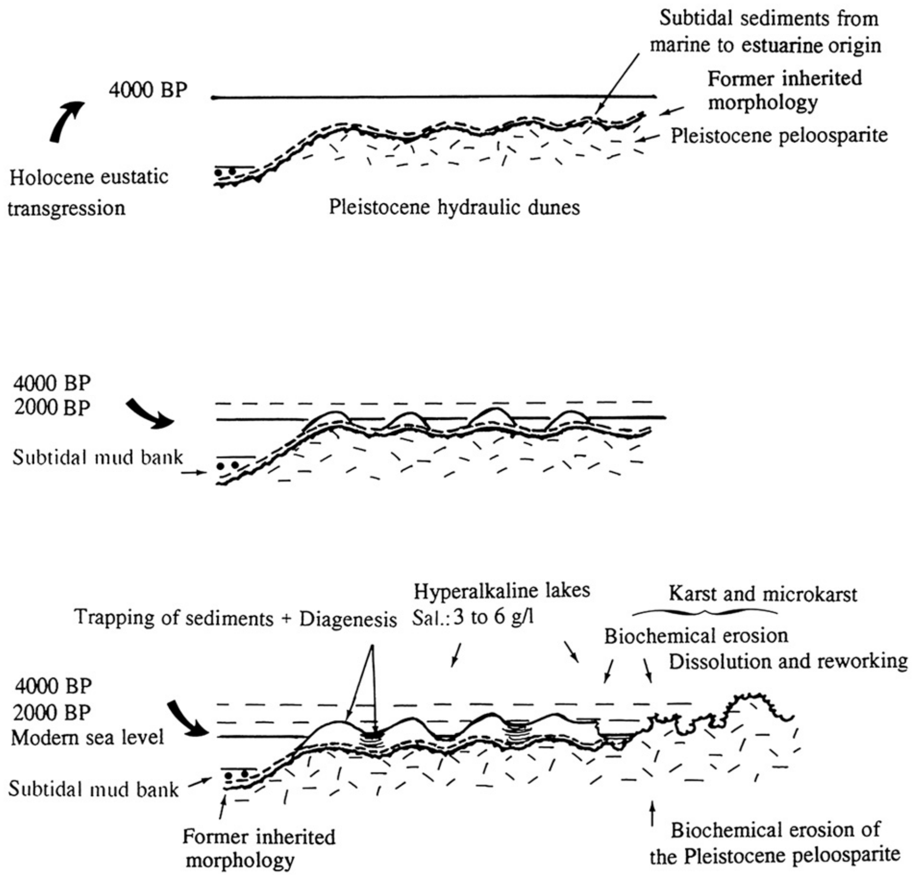

Fig. 12. Late Holocene evolution of the tidal flats, western Andros Island deduced from Fig. 11. (Top) Mid-Holocene transgression of the northwestern Andros Island, at 4000 years BP. (Middle) the same area is covered by carbonate mangroves in a sub- to intertidal zone between 2000–3000 years BP. (Bottom) Modern mangrove swamp carbonates in an inter- to supratidal zone.

permitted the trapping of this mud in the tidal flats (Fig. 12).

5.3.4. Development of the present-day cyclonic system in the Bahamas:

The supratidal Bahamian hummocks are formed by the pile-up of intercalated marks left by hurricanes. For *Casuarina* Cape (altitude about 1.5 m), these occur from 1670 years BP at −0.7 m from a core top dated by Cloud (1962), and dated in this work from 2030 years BP at station 35 at −0.22 to −0.32 m from core top in an infilled estuary.

On the north bank of Wide Opening, a core taken from the wet mangrove with cyanobacterial mats was dated between 3000 to 3500 years BP, corresponding to the beginning of a tropical climate undergoing disturbances such as tropical cyclones and hurricanes. In addition, in the zone of the Pelican estuary, a number of dates indicate an important sedimentary influx; more than 80 cm in the last 2000 years. The age of core #58735, in particular, seems to indicate a rapid influx that took place recently. This could be a record of a rapid accretion by sediment transport and deposition linked to very high-energy mechanisms (hurricanes and cyclones), confirming our conclusions about the evolution of geomorphologic and sedimentologic features. But the stagnation of water tables (almost fresh water) causes biochemical and mostly chemical alteration of the far north hurricane trails of the tidal flats.

Detailed sedimentological analysis of the Andros model allows calculation of the age of the present-day high-energy climatic system development in the Bahamas. The oldest cyclonic marks that can be recognized so far seem to indicate that this climatic system was already in place about 2000 years BP.

Therefore, the general geomorphological features are constant throughout this time, i.e. (a) — the development of cyclonic levees initiated by Pleistocene sedimentary alignments; (b) — the continuing presence of zones in vertical series that have been affected by lacustrine environment; (c) — the thinning of each laminae representing a hurricane on the side opposite to its origin; (d) — a low and undulating substratum, and finally (e) — the sediment source of the tidal flat from the subtidal talus, on the border and the lee side of the tidal flat, but on the stoss side of hurricane tracks.

The maximum rate of 0.5 mm/yr has allowed the build-up of this "V" shaped sedimentary deposit with a hurricane-transported Didemnid micritic facies, first in intertidal depths between 3500 and 2000 years BP and then in a supratidal regime, related to the slow lowering of the marine level.

6. Conclusions

The climatic consequences show that the sedimentary processes (accretion and diagenesis) controlled by high-energy phenomena (tropical cyclones and hurricanes), seem to have followed a Mid-Holocene transgression culminating about 3000 years BP and have become established in the Bahama archipelago beginning between 2500 and 2000 years BP.

Contrary to the generally accepted ideas, the Mid-Holocene sea-level on the Great Bahama Bank was higher than the present-day and situated at about +1.5 m. The present-day geomorphological system of the tidal flat on western Andros Island has existed since about 5000 years BP with paleo-estuaries in the same place as those of today.

The geological consequences are important because this Mid-Holocene sea-level highstand shows that the present-day zones affected by dolomitization are being slowly emerged by relative sea-level fall and at a constant rate, more or less, in hurricane or tropical cyclones frequency, illustrating a new dolomitization model in a wet tropical environment in relation to evaporation and emergence.

The radiocarbon dates from different cores allow calculation of sedimentation rates and show that on the tidal flat: (1) the sedimentary material is brought in and not precipitated *in situ*; (2) the sedimentation rate is low in a tidal basin (most distant sedimentological feature from the marine environment), and the rate of maximum accretion takes place on the banks of the estuaries; (3) this sedimentary deposit comes from a marine environment; (4) the constant decrease in carbonate sedimentation rate from 5000 years BP to 0 year BP is in relation with the diminution of accommodation because of the existence of a higher Mid-Holocene sea-level on the Great Bahama Bank.

The data presented herein suggest that the tidal flats are being eroded on the northwest coast and have vertically accreted, not prograded.

Acknowledgments

I thank the Centre des Faibles Radioactivités, the Laboratoire de Radiocarbone de l'Université Claude-Bernard in Lyon and the Centre Scientifique de Monaco for performing the radiocarbon dating, as well as Elf Aquitaine and TOTAL for scientific support, and D. S. Gorsline, Professor Emeritus from the University of

Southern California, and P.-A. Bourque, Professor in the University Laval in Québec for revision of the English manuscript. Previous encouragement by Professor Eugen Seibold is also gratefully acknowledged.

References

Baker, R.G.V., Haworth, R.J., 1997. Further evidence from relic shellcrust sequences for a late Holocene higher sea level for eastern Australia. Mar. Geol. 141, 1–9.

Bard, E., Arnold, M., Hamelin, B., Tisnerat-Laborde, N., Cabioch, G., 1998. Radiocarbon calibration by means of mass spectrometric $^{230}Th/^{234}U$ and ^{14}C ages of corals: an updated database including samples from Barbados, Mururoa and Tahiti. Radiocarbon 40 (3), 1085–1092.

Beaman, R., Lacombe, P., Carter, R.M., 1994. New evidence for the Holocene sea-level high from the inner shelf, central Great Barrier Reef, Australia. J. Sediment. Res. A64 (4), 881–885.

Belknap, D.F., Kraft, J.C., 1977. Holocene relative sea-level changes and coastal stratigraphic units on the northwest flank of the Baltimore Canyon Trough geosyncline. J. Sediment. Petrol. 47, 610–629.

Blum, M.D., Misner, T.J., Collins, E.C., Scott, D.B., Morton, R.A., Aslan, A., 2001. Middle Holocene sea-level rise and highstand at +2 m, central Texas coast. J. Sediment. Res. 71 (4), 581–588.

Boardman, M., Neumann, A.C., Rasmussen, K.A., 1989. Holocene sea level in the Bahamas. In: Myroye, J.E. (Ed.), Proc. 4th Symposium on the Geology of the Bahamas. College of Finger Lakes Bahamian Field Station, Fort Lauderdale, FL, pp. 45–52.

Bond, G., Showers, W., Cheseby, M., Lotti, R., Almasi, P., de Menocal, P., Priore, P., Cullen, H., Hajdas, I., Bonani, G., 1997. A pervasive millennial-scale cycle in north Atlantic Holocene and glacial climates. Science 278, 1257–1285.

Bourrouilh-Le Jan, F.G., 1973. Les dolomies et leurs genèses. Bull. Cent. Rech. Pau-SNPA 7 (1), 111–135 (7 fig., 4 pl).

Bourrouilh-Le Jan, F.G., 1974a. Données géomorphologiques sur la région de Fresh Creek, Ile Andros, Bahama. Mar. Geol. 16, 213–235.

Bourrouilh-Le Jan, F.G., 1974b. Sédimentologie et pétrographie sédimentaire du Pléistocène bahamien: Région de Fresh Creek, Ile Andros, Bahama. VIIème Conf. géol. Caraïbes, Dir. Mines, Min. Ind. et Rech. Ed., BP 448, Guadeloupe, Antilles françaises, 285–292.

Bourrouilh-Le Jan, F.G., 1976. Sédimentation carbonatée littorale, île Andros (Bahama). Film 16 mm, couleurs, son optique, 300 m, 27 mm, 1976. Serv. Film Rech. Scientif., CERIMES, 6 avenue Pasteur, 92170 Vanves France.

Bourrouilh-Le Jan, F.G., 1978. Rôle des ouragans et des cyclones tropicaux sur la sédimentation carbonatée: la plaine d'estran de l'Ouest d'Andros (Bahama). Interférences de la climatologie, de l'hydrologie et de la diagenèse. C.R. Acad. Sci. Paris, Sér., D. 287, 907–910.

Bourrouilh-Le Jan, F.G., 1979. Hurricanes and rainfalls: a key for dolomitization in the Tidal Flats of western Andros, Bahamas. Abstr., S.E.P.M. Research Symposium. SEPM-AAPG Round table, Houston, p. 423.

Bourrouilh-Le Jan, F.G., 1980. Hydrologie des nappes d'eau superficielles de l'île Andros, Bahama. Dolomitisation et diagenèse de plaine d'estran en climat tropical humide. Bull. Cent. Rech. Explor. Prod. Elf-Aquitaine, Pau 4 (2), 661–707 (20 fig., 9 tabl).

Bourrouilh-Le Jan, F.G., 1981. Hurricane Trails : Supratidal Mud Bodies on the tidal Flats of western Andros, Bahamas. Geometry and Mineralogy. Penrose Conference on Controls of Platform Carbonate Evolution. Geol. Soc. America, Capri, September 1981. Abst. Poster.

Bourrouilh-Le Jan, F.G., 1982. Géométrie et minéralogie des corps sédimentaires dans une mangrove carbonatée sous l'influence des ouragans, île Andros, Bahamas. Mém. Soc. Géol. Fr., N.S. (144), 77–92.

Bourrouilh-Le Jan F.G., 1990. Diagenèse des carbonates de plates-formes, récifs et mangroves en Atlantique et Pacifique. Contrôle de la diagenèse par les variations thermo-glacio-eustatiques d'émersion–submersion. Aragonite, calcite, dolomite. Thèse, Doct. d'Etat-Univ. P.-et-M.-Curie/Paris VI, 216 p., avec 2 documents annexes.

Bourrouilh-Le Jan, F.G., 1993. A Mid-Holocene sea-level stand higher than now, on the Bahama platforms and the setting up of a hurricane regime on the North-American SE coast. UNESCO-IUGS, Climates of the Past, Ocas. Public. CIFEG 1993/25, p. 18.

Bourrouilh-Le Jan, F.G., 1996. Plates-formes carbonatées et atolls du Centre et Sud Pacifique. Stratigraphie, sédimentologie, minéralogie et géochimie. Diagenèses et Émersionbs: Aragonite, calcite, dolomite, bauxite et phosphate. Doc. B.R.G.M., vol. 249. 365 pp.

Bourrouilh-Le Jan, F.G., 1998. The role of high-energy events (hurricanes and/or tsunamis) in the sedimentation, diagenesis and karst initiation of tropical shallow water carbonate platform and atolls. Sediment. Geol. 118, 3–36.

Cazenave, A., 1999. Les variations annuelles du niveau moyen de la mer. C. R. Acad. Sci., Ser. 2, Sci. Terre Planètes 329, 457–469.

Chen, J.L., Wilson, C.R., Chambers, D.P., Nerem, R.S., Tapley, B.D., 1998. Seasonal global water mass budget and mean sea level variations. Geophys. Res. Lett. 25, 3555–3558.

Clark, J.A., Ligle, C.S., 1979. Predicted relative sea-level changes (18,000 years BP to present) caused by late-glacial retreat of the Antarctic retreat ice sheet. Quat. Res. 11, 279–298.

Clark, J.A., Farrel, W.E., Peltier, W.R., 1978. Global changes in sea level: a numerical calculation. Quat. Res. 9, 265–287.

Cloud, P.E., 1962. Environment of calcium carbonate precipitation deposition, West of Andros Island, Bahamas. U.S. Geol. Surv. Prof. Pap. 50, 1–138.

Cry, G.W., 1965. Tropical cyclones of the North Atlantic Ocean tracks and frequencies of hurricanes and tropical storms, 1871–1963. U.S. Weather Bureau Technical Paper, vol. 55. U.S. Government Printing Office, Washington, D.C. 148 pp.

Curray, J.R., 1960. Sediments and history of Holocene transgression, continental shelf, northwest Gulf of Mexico. In: Shepard, F.P., Phleger, F.B., Van Andel, T.H. (Eds.), Recent Sediments Northwest Gulf of Mexico. Amer. Assoc. Petrol. Geol. Bull. 221–226.

Curray, J.R., 1961. Late Quaternary sea level: a discussion. Geol. Soc. Amer. Bull. 72, 1707–1712.

Dechamps, R., Guillet, B., Schwartz, D., 1988. Découverte d'une flore forestière mi-Holocène (5 800–3 100 B.P.) conservée in situ sur le littoral ponténégrin (R. P. du Congo). C. Acad. Sci. Paris, t. 306, Sér. II, pp. 615–618.

Denniston, R.F., Gonzalez, L.A., Asmerom, Y., Baker, R.G., Reagan, M.K., Bettis III, E.A., 1999. Evidence for increased cool season moister during the middle Holocene. Geology 27 (9), 815–818 (3 figs., 2 tb).

Dix, G.R., Kyser, K., 2000. Punctuated environmental change along the Holocene (<6 ka) bank margin of south-west Exuma Sound, Bahamas. Sedimentology 47, 421–434.

Dupuit, J., 1848–1863. Études théoriques et pratiques sur le mouvement des eaux dans les canaux découverts et à travers les terrains perméables. Dunod, Paris.

Fleming, K., Johnston, P., Zwartz, D., Yokoyama, Y., Lambeck, K., Chappell, J., 1998. Refining the eustatic sea-level curve since the Last Glacial Maximum using far- and intermediate-field sites. Earth Planet. Sci. Lett. 163, 327–342.

Fletcher, C.H., Jones, A.T., 1996. Sea-level highstand recorder in Holocene deposits on Oahu, Hawaii. J. Sediment. Res. 666, 632–641.

Flood, P.G., Frankel, E., 1989. Late Holocene sea level indicators from eastern Australia. Mar. Geol. 90, 193–195.

Frazier, D.E., 1974. Depositional episodes: their relationship to the Quaternary stratigraphic framework in the northwestern portion of the Gulf basin, Austin. The University of Texas, Bureau of Economic Geology, Geological Circular, 74-1. 28 pp.

Friedman, G.M., 1994. Great Bahama Bank aragonite muds: mostly inorganically precipitated, mostly exported — discussion. J. Sediment. Res., Sect. A, Sediment. Pet. Proc. 64, 398–399.

Gebelein, C.D., 1974. Guidebook for modern Bahamian platform environments: field trip. Geological Society of American Annual Meeting, Boulder, CO, 93 p.

Gebelein, C.D., 1975. Holocene sedimentation and stratigraphy, southwest Andros Island, Bahamas. 9th Intern. Congr. Sedimentology, Nice, Thème 5, t. 1, pp. 193–198.

Gebelein C.D. (1977). Dynamics of recent carbonate sedimentation and ecology. Cape Sable, Florida. Intern. Sediment. Petrogr. Ser., vol.16, Clarke, Purser and Wagner, edit., Leiden, Brill, 120 p., 52 fig., 8 pl.

Gebelein, C.D., 1978. Stratigraphy of Holocene Deposit, North-West Andros island (Bahamas). 6th Meet. Carbonate Sedimentol. (Liverpool, 3–7 January 1978). Abstract.

Gebelein, C.D., Hoffman, P., 1973. Algal origin of dolomite laminations in stromatolitic limestone. J. Sediment. Petrol. 43, 603–613.

Gebelein, C.D., Steinen, R.P., Garret, P., Hoffman, E.J., Queen, J.M., Plummer, L.N., 1980. Subsurface dolomitization beneath the tidal flats of central west Andros Island, Bahamas. In: Zenger, Dunham, Ethington (Eds.), Concepts and Models of Dolomitization. SEPM Spec. Publ., vol. 28, pp. 31–49.

Ghyben, B.W., 1888–1889. Nota in verband de voorgenomen putboring Nabij Amsterdam. Tijdschrift van het Koninklijk Instituut van Ingenieurs. The Hague 21.

Ginsburg, R.N., Hardie, L.A., 1975. Tidal and storm deposits, northwestern Andros Island, Bahamas. In: Ginsburg, R.N. (Ed.), Tidal Deposits. A Case Book of Recent Examples and Fossils Counterparts. Springer, Berlin.

Goodwin, I., 1998. Did changes in Antarctic ice volume influence late Holocene sea-level lowering ? Quat. Sci. Rev. 17, 319–332.

Gornitz, V., Seeber, L., 1990. Vertical crustal movements along the East coast, North America, from historic and late Holocene sea-level data. Tectonophysics 178, 127–150.

Grossman, E.E., Fletcher III, C.H., 1998. Sea level higher than present 3,500 years ago on the normative main Hawaiian Islands. Geology 26 (4), 363–366 (3 figs., 1 tb).

Hardie, L.A., 1977. Sedimentation on the modern carbonate tidal flats of northwest Andros Island, Bahamas. Johns Hopkins Univ., Stud. Geol. 22 (202 pp.).

Hearty, P.J., Neumann, A.C., Kaufman, D.S., 1998. Chevron ridges and runup deposits in the Bahamas from storms late in oxygene-isotope substage 5e. Quat. Res. 50, 309–322.

Herzberg B., 1901. Die wasserversorgung einiger Nordseebäder. Journ. Gasbeleuchtung und Wasserversorgung, 44, 815–819 und 842–844.

Hubbard, D.K., Zankl, H., Van Heerden, I., Gill, I.P., 2005. Holocene reef development along the northeastern St. Croix shelf, Buck Island, U. S. Virgin Islands. J. Sediment. Res. 75 (1), 97–113.

Ingolfsson, O., Hjort, C., Berkman, P.A., Bjork, S., Colhoun, E., Goodwin, I.D., Hall, B., Hirikawa, K., Melles, M., Moller, P., Prentice, M.L., 1998. Antarctic glacial history since the last glacial maximum: an overview of the record on land. Antarct. Sci. 10, 326–344.

Jedoui, Y., Kallel, N., Fontugne, M., Ben Ismail, H., M'Rabet, A., Montacer, M., 1998. A high relative sea-level stand in the middle Holocene of southeastern Tunisia. Mar. Geol. 147, 123–130.

Kindler, P., Strasser, A., 2000. Paleoclimatic significance of co-occuring wind-and water-induced sedimentary structures in the last-interglacial coastal deposits from Bermuda and the Bahamas. Sediment. Geol. 131, 1–7.

Lambeck, K., 1993. Glacial rebound and sea level change: an example of a relationship between mantle and surface processes. Tectonophysics 223, 15–37.

Leuschner, D.C., Sirocko, F., 2000. The low-latitude monsoon climate during Dansgaard–Oeschger cycles and Heinrich Events. Quat. Sci. Rev. 19, 243–254.

Lévy, A., 1977. Révision micropaléontologique des *Soritidae* actuels bahamiens. Un nouveau genre: *Androsina*. Bull. Cent. Rech. Explor. Prod. Elf-Aquitaine 1 (2), 393–449.

Lévy, A., 1991. Peuplements actuels et thanatocoenoses à *Soritidae* et *Peneroplidae* des Keys de Floride (USA). Oceanol. Acta 14 (5), 515–524.

Lévy, A., Mathieu, Poignant, A., Rosset-Moulinier, M., 1988. Les *Soritidae* et les *Peneroplidae* dans les biofaciès de la plate-forme des Bahamas. Rev. Paléobiol., Benthos 86 (2), 833–841.

Lidz B.H., Shinn E.A., Hansen M.E., Halley R.B., Harris M.W., Locker S.D., Hine A.C., 1997. Maps showing sedimentary and biological environments, depth to Pleistocene bedrock, and Holocene sediment and reef thickness from Molasses Reef to Elbow Reef, Key Largo, South Florida. Miscellaneous investigations series, U. S. G. S. Investigative Series Map#I-2505, in coop. Univers. South Florida, 3 sheets.

Lowenstam, H.A., Epstein, S., 1957. On the origin of sedimentary aragonite needles of the Great Bahama Bank. J. Geol. 65, 364–375.

Macintyre, I.G., Reid, R.P., 1992. Comment on the origin of Bahamian aragonite muds: a picture is worth a thousand words. J. Sediment. Petrol. 62, 1095–1097.

Macintyre, I.G., Reid, R.P., Steineck, R.S., 1996. Growth history of stromatolites in a Holocene fringing reef, Stocking Island, Bahamas. J. Sediment. Res. 66 (1), 231–242.

Milliman, J.D., 1994. Great Bahama Bank aragonite muds: mostly inorganically precipitated, mostly exported — reply. J. Sediment. Res., Sect. A Sediment. Pet. Proc. 64 (4), 922.

Milliman, J.D., Freile, D., Steinen, R.P., Wilber, J., 1993. Great Bahama Bank aragonite muds: mostly inorganically precipitated, mostly exported. J. Sediment. Petrol. 63 (4), 589–595.

Minster, J.F., Cazenave, A., Serafini, Y.V., Mercier, F., Gennero, M.-C., Rogel, P., 1999. Annual cycle in mean sea level from Topex-Poseidon and ESR-1: inference on the global hydrological cycle. Glob. Planet. Change 20, 57–66.

Moustafa, Y.A., Pätzold, J., Loya, Y., Wefer, G., 2000. Mid-Holocene stable isotope record of corals from the northern Red Sea. Int. J. Earth Sci. 88, 742–751.

Nakada, M., Lambeck, K., 1988. The melting history of the Late Pleistocene Antarctic ice sheet. Nature 333, 36–40.

Nelson, H.F., Bray, E.E., 1970. Stratigraphy and history of the Holocene sediments in the Sabine-High Island area, Gulf of

Mexico. In: Morgan, J.P. (Ed.), Deltaic Sedimentation, Modern and Ancient. Soc. Econ. Miner., Spec. Publ., vol. 15, pp. 48–77.
Newell, N.D., Rigby, J.K., 1957. Geological studies on the Great Bahama Bank. In Regional aspects of Carbonate Deposition. In: Le Blanc, R.J., Breeding, J.G. (Eds.), Soc. Econ.Pal. and Min., Spec. Publ., vol. 5, pp. 15–72.
Newell, N.D., Imbrie, J., Purdy, E.G., Thurber, D.L., 1959. Organism communities and bottom facies, Great Bahama Bank. Bull. Am. Mus. Nat. Hist. 177–228.
Neumann, A.C., Land, L.S., 1975. Lime mud deposition and calcareous algae in the Bight of Abaco: a budget. J. Sediment. Petrol. 45, 763–786.
Neumann, C.J., Cry, G.W., Caso, E.L., Kerr, J.D., 1978. Tropical Cyclones of North Atlantic Ocean, 1871–1977. Stock #003-1 7-0042502, National Climatic Center, U. S. Government Printing Office, Asheville, N. C.
Pardi, R.R., Newmann, W.S., 1987. Late Quaternary sea levels along the Atlantic coast of North America. J. Coast. Res. 3 (3), 325–330.
Parkinson, R.W., 1989. Decelerating Holocene sea-level rise and its influence on southwest coastal evolution: a transgressive/regressive stratigraphy. J. Sediment. Petrol. 59, 960–972.
Peltier, W.R., 1998. Postglacial variations in the level of the sea: implications for the climate dynamics and solid earth geophysics. Rev. Geophys. 36, 603–689.
Penland, S., McBride, R.A., Williams, S.J., Boyd, R., Suter, J.R., 1991. Effects of sea level rise on the Mississippi River delta plain. In: Kraus, N.C., Gingerich, K.J., Kriebel, D.L. (Eds.), Coastal Sediments '91. Amer. Soc. Civ. Engineers, New York, pp. 1248–1264.
Posamentier, H.W., Allen, G.P., 1999. Siliciclastic sequence stratigraphy — concepts and applications. SEPM Concepts in Sedimentology and Paleontology, vol. 7. 210 pp.
Purdy, E.G., 1963. Recent calcium carbonate facies of the Great Bahama Bank. 1. Petrography and reaction groups. J. Geol. 71 (3), 334–355.
Rankey, E.C., 2002. Spatial patterns of sediment accumulation on a Holocene carbonate tidal flat, northwest Andros Island, Bahamas. J. Sediment. Geol. 72 (5), 591–601.
Rankey, E.C., Enos, P., Steffen, K., Druke, D., 2004. Lack of impact of hurricane Michelle on tidal flats, Andros Island, Bahamas: integrated remote sensing and field observations. J. Sediment. Res. 74 (5), 654–661.
Robbins, L.L., Blackwelder, P.L., 1992. Origin of whitings: a biologically induced non-skeletal phenomenon. Geology 20, 464–467.
Robbins, L.L., Tao, Y., Evans, C.A., 1997. Temporal and spatial distribution of whitings on Great Bahama Bank and a new lime mud budget. Geology 25 (10), 947–950.
Rodriguez, A.B., 1999. Sedimentary facies and evolution of late Pleistocene to Recent coastal lithosomes on the east Texas shelf. Unpublished Ph.D. dissertation, Rice University, 203 p.
Scholl, D.W., Craighead Sr., F.C., Stuiver, M., 1969. Florida submergence curve revised: its relation to coastal sedimentation rates. Science 163, 562–564.
Shepard, F.P., 1963. Thirty-five thousands years of sea-level. Essays in Marine Geology in Honor to K.O. Emery, Los Angeles, California. University of Southern California Press, pp. 1–10.
Shinn, E.A., Ginsburg, R.N., Lloyd, R.M., 1965. Recent supratidal dolomite from Andros Island, Bahamas. In: Pray, L.C., Murray, R.C. (Eds.), Dolomitization and Limestone Diagenesis: A Symposium. Soc. Econ. Paleont. Miner., Spec. Publ., vol. 13, pp. 112–123.
Sowers, T., Bender, M., Labeyrie, L., Martinson, D., Jouzel, J., Raynaud, D., Pichon, J.J., Korotkevich, Y.S., 1993. A 135,000 year Vostok-SPECMAP common temporal framework. Paleoceanography 8, 737–766.
Steinen, R.P., Swart, P.K., Shinn, E.A., Lidz, B.H., 1988. Bahamian lime mud: the algae didn't do it. Abst. Geol. Soc. Amer., Abstract with Programm, vol. 20A, p. 209.
Stuiver, M., Grootes, P.M., Braziunas, T.F., 1995. The GISP δ18O climate record of the past 16,500 years and the role of the sun, ocean and volcanoes. Quaternary Research 44, 341–354.
Thom, B.G., Roy, P.S., 1983. Sea level change in New South Wales over the past 15,000 years. In: Hopley, D. (Ed.), Australian Sea Levels in the Last 15,000 Years: a Review. Occas. Pap. James Cook Univ, Townsville, pp. 64–84.
Thomas M.A., 1990. The impact of long term and short term sea-level changes on the evolution of the Wisconsinan-Holocene Trinity/Sabine valley system, Texas continental shelf. Unpublished Ph. D. dissertation, Houston, Texas, Rice University, 247 p.
Törnqvist, T.E., González, J.L., Newson, L.A., van der Borg, K., de Jong, A.F.M., Kurnik, C.W., 2004. Deciphering Holocene sea-level history on the U.S. Gulf Coast: a high resolution record from the Mississippi Delta. Geol. Soc. Amer. Bull. 116 (7/8), 1026–1039.
Toscano, M.A., Lundberg, J., 1998. Early Holocene sea-level record from submerged fossil reefs on the southeast Florida margin. Geology 26 (3), 255–258 (2figs., 1 tb).
Traverse, A., Ginsburg, R.N., 1966. Palynology of the surface sediments of Great Bahama Bank, as related to water movement and sedimentation. Mar. Geol. 4, 417–459.
Tushingham, A.M., Peltier, W.R., 1991. ICE-3G: a new global model of late Pleistocene deglaciation based on geophysical predictions of post-glacial relative sea-level change. J. Geophys. Res. 96, 4497–4523.
Woodroffe, C.D., Stoddart, D.R., Spencer, T., Scoffin, T.P., Tudhope, A.W., 1990. Holocene emergence in the Cook Islands, South Pacific. Coral Reefs 9, 31–39.
Zhang, H.C., Ma, Y.Z., Wünnemann, B., Pachur, H.-J., 2000. A Holocene climatic record from arid northwestern China. Palaeogeogr. Palaeoclimatol. Palaeoecol. 162, 389–401.